ENGINEERING TRANSACTIONS • *Engng. Trans.* • **44**, 3–4, 445–469, 1996
Polish Academy of Sciences • Institute of Fundamental Technological Research

ON REGULARIZATION OF PLASTIC FLOW LOCALIZATION IN A SOIL MATERIAL

M. LENGNICK (HANNOVER), T. ŁODYGOWSKI (POZNAŃ)
P. PERZYNA (WARSZAWA) and E. STEIN (HANNOVER)

Density-dependent critical state line (Cam–Clay type) model is regularized by viscoplastic formulation to assure the mathematical well-posedness of the initial Cauchy problem. In computations this reduces the so-called *Primary Mesh Dependence* which is defined in the paper. Several numerical examples of two-dimensional plane strain pillar problem confirm the validity of the proposed formulation and its usefulness in numerical calculations.

1. INTRODUCTION

In many practical engineering problems the knowledge of post-critical behaviour of the system under consideration significantly helps to predict its safety. The detailed information on both global (e.g. force-displacement relations) and local (e.g. the distributions of strains) levels are very important. The localization of deformations, which is experimentally a very well observed physical phenomenon, is characterized by appearing of large strains in relatively narrow zones of the specimen. This phenomenon nearly always accompanies the failure in ductile (metals, polymers) as well as in brittle materials (concrete, ceramics), including soils. The width and directions of the localized zones depend significantly not only on the material parameters but also upon the shape of the specimen and the initial and boundary conditions. One should also stress here two important qualitative results, and namely:

- the width of localization, being very narrow in some experiments, is always finite, even for very fast processes,
- the width and directions of the zones of concentrated strains significantly depend on the type of loading and its velocity. The localization patterns are usually different for quasi-static and for dynamic types of deformations.

To present the motivation which is based on the experimentally observed physical facts and to define the background of this presentation, several levels of the treatment of the localization are presented in Box 1.

Box 1

Experimental Results

Mathematical Formulation of the observed Physical Phenomena

- Statistical Mechanics
- Microlevel Description
- **Continuum Mechanics Description**
  - Continuum Damage Mechanics
  - Fracture Mechanics
  - **Plasticity with softening**
    - Smeared Crack Models
    - Higher Gradients Models
    - Embedded Models
    - Cosserat Models
    - **Rate–Dependent Models**
    - others

If we concentrate on the continuum-mechanical basis, one can notice that the phenomenon of localization which starts from the microlevel, is not directly observable on the purely phenomenological level of description. It seems to be natural that we have to introduce the additional information which allow us to model more precisely the problem of nucleation and growing of microdefects which are macroscopically observable as a localization.

One of the used descriptions is based on the rate-independent plasticity and introduces the strain-softening effect which smeares out the localization strains over the certain domain. In fact, the softening modulus used in this formulation is not measure-invariant in the sense that it is dependent on the strain measure. This approach drives, in turn, to apply materials which do not satisfy the Drucker material stability conditions.

Finally, if one would restrict the attention to the strain-softening rate-independent materials, the local Cauchy problem as well as the initial-boundary value problems become not well-posed after the critical loading has been reached. The loss of ellipticity or hyperbollicity of the system of the govern-

ing equations which can be associated with the localization phenomenon, can appear as a result of lack of normality of the plastic flow (nonassociated flow) or through the introduction of the strain softening effects.

The analysis of the localization phenomena has been performed by many authors, beginning with the works of HILL [11], MANDEL [22], RUDNICKI and RICE [33] or RICE [32]. Two important questions must be answered before solving any initial-boundary value problems with localization. First, on the level of mathematical modelling one has to be able to predict when, where and in which direction the localization zones will appear and what will be their width. Also, the problem of well-posedness has to be the subject of interest. Second, from the viewpoint of numerical simulation, one should not avoid the discussion on mesh-dependence (see for example [20]). This is particularly important because in some presentations, the notions of unusually high mesh sensitivity of the results of calculations appear.

In Box 1 we have indicated different possible treatments of the problems of localization of plastic flow which exhibits softening. They are different from each other, however all of them introduce implicitly or explicitly the length scale that plays the role of a regularization parameter. This ensures the well-posedness of the so-called abstract Cauchy problem which is the necessary condition of uniqueness of the solution of the initial boundary value problem (IBVP); e.g. see [15].

Among other possible methods of regularization which are briefly indicated in Box 1, we will use the viscoplastic one.([1]) We will concentrate our attention on the regularized formulation and numerical implementation of the rock/soil/clay model of the material of the so-called critical state line type. Two-dimensional plane strain examples without and with regularization are presented and discussed. The idea of the primary and secondary mesh dependence is introduced and numerically verified. The numerical results are obtained by means of the user subroutine option UMAT in ABAQUS program.

The aim of the paper is to propose, for IBVP which use the soil-like materials, the viscoplastic method of regularization, in particular for plastic flow localization which accompanies the dynamical load cases. Another goal is to discuss the numerical aspects of sensitivity of the results to the finite element mesh used in computations when the softening occurs, see also ŁODYGOWSKI [20]. The method which we have proposed here guarantees the stability and

([1]) For a thorough discussion of the concept of viscoplastic regularization for polycrystalline solids see PERZYNA [29, 30], and for geological materials DUSZEK–PERZYNA *et al.* [7]. The review of the theory and numerical treatment of the localization phenomena in geomaterials will be presented by DUSZEK–PERZYNA *et al.* in [8].

uniqueness of the obtained results; being not purely mathematical, it has also the physical arguments in the definition of the model parameters.

The paper is organized as follows. First, we present the rate-independent soil model to show in examples the significant and not acceptable mesh dependence of the obtained numerical results. Then, after formulation of the primary and secondary mesh dependence, the viscoplastic regularization of the plastic flow localization is presented. Next, we specify the consistent matrices for 2–D plane strain cases. Numerical studies of pillar examples which show a significant reduction of the primary mesh sensitivity and the conclusions close the paper.

2. Rate–independent formulation

2.1. Notation

Let us introduce the well-known multiplicative decomposition of the deformation gradient $\mathbf{F}$ in the form (see Lee [16])

$$\mathbf{F} = \mathbf{F}^e \mathbf{F}^p, \tag{2.1}$$

where $\mathbf{F}(\mathbf{X}, t) = \partial \mathbf{x}(\mathbf{X}, t)/\partial \mathbf{X}$ and $\mathbf{F}^e$, $\mathbf{F}^p$ are the so-called elastic and plastic deformation gradients, respectively. The velocity gradient $\mathbf{L}$ can be then decomposed into the elastic and plastic parts

$$\mathbf{L} = \mathbf{L}^e + \mathbf{L}^p, \tag{2.2}$$

and each of them can be further presented as a sum of its symmetric and nonsymmetric parts; for example, the elastic part is written as

$$\mathbf{L}^e = \mathbf{D}^e + \mathbf{W}^e. \tag{2.3}$$

The symmetric part of $\mathbf{L}$, namely $\mathbf{D}$, represents the stretching tensor and $\mathbf{W}$ the spin tensor.

Next, let us define the bar form of the selected second order tensors with respect to the group of rotations $\mathbf{Q}^e$ by the following transformations (see Gurtin [10])

$$\overline{\mathbf{T}} = \mathbf{Q}^{eT}\,\mathbf{T}\,\mathbf{Q}^e, \qquad \overline{\mathbf{D}} = \mathbf{Q}^{eT}\,\mathbf{D}\,\mathbf{Q}^e, \tag{2.4}$$

where $\mathbf{T}$ represents the Cauchy stress tensor and $\mathbf{Q}^e(t)$ defines the group of time-dependent rotations through the initial value problem

$$\dot{\mathbf{Q}}^e = \mathbf{W}^e\,\mathbf{Q}^e, \qquad \text{with} \qquad \mathbf{Q}^e(0) = \mathbf{1}, \tag{2.5}$$

where **1** is the identity tensor and $(\ )^T$ denotes transposition. This rotational-neutralized (pull-back) tensorial quantities which are introduced here (see also GURTIN [10]) will be used to define the convenient framework for integration of the constitutive model. With these definitions, the time derivative of the Cauchy stress tensor satisfies the equation

$$\dot{\mathbf{T}} = \mathbf{Q}^{eT}\,\mathbf{T}^{\nabla e}\,\mathbf{Q}^{e} \equiv \overline{\mathbf{T}}^{\nabla e}, \tag{2.6}$$

and is objective in the sense of material frame-indifference (cf. TRUESDELL and NOLL [38]), i.e. is invariant with respect to any superposed rigid motion.

2.2. Rate-independent material model

Let us summarize some basic assumptions of an elastic-plastic model of soil-like material with the yield conditions which depend upon the hydrostatic pressure and changes of porosity. This material model belongs to the so-called critical state models (see WOOD [39]) and was originally introduced by PIETRUSZCZAK and MRÓZ in [31] to model granular and rock materials. Let us assume also that the yield condition is a function of stresses and depends on the irreversible part of porosity or density variation η, which is the internal state variable. Hardening and/or softening behaviours are introduced through the evolution of this internal scalar state variable. The model which is presented intends to simulate, contrary to the known Cam-Clays, the constitutive behaviour which is not restricted to the purely cohesionless materials. Similarly to the other Cam-Clay-type models, yielding depends on the hydrostatic pressure and critical state line separates two regions of different behaviours: hardening or softening (for detailed discussion see WOOD [39], LORET [21], DRESCHER [6], ADACHI and OKA [2] *et al.*). In this model, on the so-called "dry" side the material dilates and, in a consequence softens, while on the so-called "wet" side it hardens what accompanies compaction. Main property of this model is that on the critical state line the material can yield at constant shear stress with no volume changes. The other important property is that the yield is influenced by the mean principal stress. We restrict our attention to the one-phase material model.

The relative bulk density, that is the introduced scalar variable, is defined by

$$\eta = \frac{\varrho}{\varrho_0}, \tag{2.7}$$

where ϱ denotes the mean bulk density, and ϱ_0 the intrinsic material bulk density at a reference, in general, unloaded configuration, respectively. The

porosity which could be defined as

$$\beta = \frac{V_v}{V_t}, \tag{2.8}$$

in which V_v and V_t denote the volume of voids and the total volume of the representative specimen, can play also a similar role of an internal state variable. η can be expressed also as

$$\eta = \frac{V_m}{V_t} = \frac{V_t - V_v}{V_t} = 1 - \beta, \tag{2.9}$$

where additionally V_m describes the material volume. The change of the internal state variable η is given by

$$\dot{\eta} = \frac{\dot{\varrho}}{\varrho_0}. \tag{2.10}$$

From the continuity condition

$$\dot{\varrho} + \varrho \operatorname{div} \mathbf{v} = 0, \tag{2.11}$$

where $\mathbf{v}$ denotes the velocity, we arrive at

$$\dot{\varrho} = -\varrho \operatorname{tr}\left(\overline{\mathbf{D}}\right), \tag{2.12}$$

and after the decomposition of $\overline{\mathbf{D}}$ into elastic and plastic parts we obtain

$$\dot{\eta} = \underbrace{-\eta \operatorname{tr}(\mathbf{D}^e)}_{\dot{\eta}^e} \underbrace{- \eta \operatorname{tr}(\mathbf{D}^p)}_{\dot{\eta}^p}. \tag{2.13}$$

The second term of the right-hand side of (2.13) $\dot{\eta}^p$ is the irreversible rate of change of porosity. Finally, the set of equations for the rate-independent material model expressed in transformed form with respect to rotation group $\mathbf{Q}$ is as follows:

- Evolution equation for the Cauchy stresses

$$\overset{\nabla}{\overline{\mathbf{T}}} = \mathbf{C} : \left(\overline{\mathbf{D}} - \overline{\mathbf{D}}^p\right), \tag{2.14}$$

where $\mathbf{C} = 2G\mathbf{I} + (K - (2/3)G)\mathbf{1} \otimes \mathbf{1}$ is an elastic material tensor; $\overline{\mathbf{D}}^p$ is the tensor of the rate of plastic deformation which has the form

$$\overline{\mathbf{D}}^p = \langle \dot{\lambda} \rangle \overline{\mathbf{N}}, \qquad \overline{\mathbf{N}} = \frac{\partial f}{\partial \overline{\mathbf{T}}}, \tag{2.15}$$

and where

$$\langle \dot{\lambda} \rangle = \begin{cases} \dot{\lambda} & : \quad \text{if} \quad f = 0 \quad \text{and} \quad \overline{\mathbf{N}} : \mathbf{C} : \overline{\mathbf{D}} > 0, \\ 0 & : \quad \text{if} \quad f \neq 0 \quad \text{or} \quad f = 0 \quad \text{and} \quad \overline{\mathbf{N}} : \mathbf{C} : \overline{\mathbf{D}} \leq 0. \end{cases}$$

f is the yield function which depends, like in the critical state line type models, upon deviatoric stresses, mean pressure and also on the introduced internal state variable η and its evolution (2.13). The yield function is assumed in the form

$$f = \hat{f}(S, p, c) = (p - c)^2 + \frac{1}{2}\left(\frac{S}{d}\right)^2 - \left(\frac{\mu_c c}{d}\right)^2 \leq 0, \tag{2.16}$$

and the following notations are used:

$$S = \sqrt{\overline{\mathbf{S}} : \overline{\mathbf{S}}}, \qquad \overline{\mathbf{S}} = \operatorname{dev}\left(\overline{\mathbf{T}}\right), \qquad p = -\operatorname{tr}\left(\overline{\mathbf{T}}\right)/3. \tag{2.17}$$

The geometrical interpretation of this yield function in (S, p) space and its evolution are discussed in many papers, e.g. see DRESCHER [6]. Also following this work we have adopted the material function c in the form

$$c = \hat{c}(\eta^p) = \alpha(\eta_0 + \eta^p) - c_0 \tag{2.18}$$

as well as the constant parameters α, η_0, c_0 used in numerical calculations. The system of equations which describes the constitutive relation consists of Eqs. (2.13)–(2.18). Different values of parameters c, d, μ_c define in $(S, -p)$ space different yield surfaces for which, contrary to the well documented Cam-Clay models, carrying of small tensile stresses is also possible. As an alternative of the discussed yield function f, that one which defines the modified Cam-Clay can also be used. For the latter model the yield surface consists of two elliptical segments in the (S, p) space

$$\frac{1}{\psi^2}\left(\frac{p}{a} - 1\right)^2 + \left(\frac{S}{Ma}\right)^2 - 1 = 0, \tag{2.19}$$

where ψ is a constant used to modify the shape of the yield surface on the "wet" side of the critical state, M is the slope of the critical state line and defines the position of the yield origin along the axis of mean pressure value p, a is a constant. The response on the "dry" side of the critical state for both the above models expressed in the (S, γ) space (γ is the shear angle) exhibits the softening behaviour, while on the "wet" side it tends to some limit value with no negative slope. The detailed discussion of the models can be found in PIETRUSZCZAK and MRÓZ [31], WOOD [39]. Some practical applications as well as the discussion of the used parameters one can find in the papers of

ADACHI and OKA [2, 3]. For rate-independent formulation one can expect the ill-posed problems and, as a consequence, in numerical computations the significant mesh sensitivity, when the yielding enforces the shrinking of the yield surface (softening) (see discussion in the work of PERZYNA [30] and also the study of DE BORST [5], SLUYS [34] and ŁODYGOWSKI [20]).

Application of the viscoplastic model to the cases involving soil materials may be criticized. But one has to agree that all the formulations indicated in Box 1, and used to describe the localization, have their advantages and drawbacks. We believe, that each soil-clay material exhibits certain amount of viscosity, and in particular for the dynamical load cases, application of viscoplasticity is justified and finds its experimental confirmation; e.g. see the works of TAVENAS *et al.* [36, 37] or LEROUEIL *et al.* [17].

For this purpose, the viscoplastic regularization is proposed to overcome the ill–posedness and to assure invariability of the type of the governing operator for the whole process, even in the post-critical states.

3. REMARKS ON MESH–DEPENDENCE

In many papers the problem of unexpected mesh-dependence of the numerical results obtained for rate-independent plasticity was discussed (for example, see [24, 29, 18]). Obviously, the numerical formulation and calculations always lead, in view of the algebraic character of the finite element technique, to approximate solutions. But for well-posed BVP the results obtained by FEM should converge to the real analytical solutions. Of course, this is true under the condition that the problems are mathematically well-posed. For ill-posed problems, one can expect extremely strong mesh sensitivity in computations and the results become meaningless.

For the purpose of this presentation let us accept now the following two definitions:

3.1. Definition 1

Mesh dependence of the first order (primary mesh dependence – PMD) is the one which follows directly from the mathematical ill-posedness of the BVP.

For ill-posed problems the uniqueness and the stability of the solution can not be proved.

As a simple consequence, when the algebraic solution based on ill-posed formulation is constructed, a serious mesh sensitivity can be easily observed

in computations. The results which are obtained in these cases exhibit different responses (particularly in the post-critical range), when the analysis is started from a changed mesh. If this kind of mesh dependence appears (PMD), it should be recognized as an effect of ill-posedness of the original mathematical formulation. For ill-posed problems the results of numerical calculations are sensitive to the finite element mesh in an unexpected manner, without the possibility of estimation of the errors that appear.

3.2. Definition 2

Mesh dependence of the second order (secondary mesh dependence SMD) reflects the well-known influence of spatial and time discretization.

For well-posed problems it approaches in the limit the analytical solution when finer meshes are used.

In this paper we are going to avoid only the *mesh dependence of the first order* PMD which, in our opinion, is the most important aim in case we are dealing with plastic localization and softening problems.

The *mesh dependence of the second order* SMD can be always avoided by applying different sophisticated numerical techniques (eg. adaptive remeshing) and can be taken into consideration only if the primary problems are satisfied. All the methods of regularization which are shown in Box 1, introduce, in fact, in a different way, a length scale parameter. It is achieved for example explicitly in embedded elements and in Cosserat formulation, or implicitly for nonlocal theories. The length scale parameter which is introduced in the formulation assures the well-posedness and the possibility of continuation of the analysis after the localization criterion is satisfied and it influences the width of the localization zones as well. For the methods mentioned above which introduce the length scale parameter, one can observe that the value is chosen almost arbitrarily (it can depend on the grain size).

It seems to be natural that, basing on the experimental observations which show that all the materials have some viscous properties, we choose PERZYNA'S viscoplasticity [26, 27, 28] as the tool of regularization.

4. RATE–DEPENDENT FORMULATION

The rate-dependent material model which is expressed in a form transformed with respect to the rotation group $\mathbf{Q}$ can be performed in the fol-

lowing manner

$$\overset{\nabla}{\mathbf{T}} = \mathbf{C} : \left(\overline{\mathbf{D}} - \overline{\mathbf{D}}^{vp}\right), \tag{4.1}$$

where $\overline{\mathbf{D}}^{vp}$ is the viscoplastic rate of deformation tensor and is assumed as [26]

$$\overline{\mathbf{D}}^{vp} = \varphi\langle\phi(S, p, \eta^p)\rangle \frac{\partial \phi}{\partial \overline{\mathbf{T}}}. \tag{4.2}$$

In the above formula φ denotes the viscosity and the associative type of plasticity is taken into account, ϕ is empirical overstress function and $\langle \cdot \rangle$ denotes the Macauley bracket which is understood as

$$\langle\phi(F)\rangle = \begin{cases} \Phi(F) & \text{if} \quad F > 0, \\ 0 & \text{if} \quad F \leq 0. \end{cases} \tag{4.3}$$

The viscosity φ is sometimes denoted by $\varphi = 1/T_m$ where T_m is relaxation time for mechanical disturbances. The relaxation time which can be used for soil-like materials is of the order of 10^{-3} s. The evolution equation for the irreversible part of the porosity changes is

$$\dot{\eta}^{vp} = -\eta \operatorname{tr}(\overline{\mathbf{D}}^{vp}). \tag{4.4}$$

The important feature derived from the viscoplastic formulation of the problem for numerical calculation is the existence, uniqueness and stability of the abstract Cauchy problem. The discussion of this problem, after the condition had been specified by KATO [14] and HUGHES, KATO and MARSDEN [13], was presented by PERZYNA in [29, 30].

Since in numerical calculations we restrict our attention to 2–D plane strain problems, let us now specify the necessary expressions which describe the constitutive model for this case. The matrix $\mathbf{C}$ takes now the form

$$\mathbf{C} = 2G\mathbf{I} + (k - G)\mathbf{1} \otimes \mathbf{1}, \tag{4.5}$$

where $k = K + (1/3)G$, and the function ϕ is expressed similarly to Eq.(2.16) as

$$\phi = (p - c)^2 + \frac{1}{2}\left(\frac{S}{d}\right)^2 - \left(\frac{\mu_c c}{d}\right)^2, \tag{4.6}$$

with the material function c given by (2.16). The viscoplastic part of the rate of deformation is now represented by

$$\overline{\mathbf{D}}^{vp} = \varphi\langle\phi(S, p, \eta^p)\rangle \left[\frac{S}{d^2}\overline{\mathbf{n}} - (p - c)\mathbf{1}\right], \tag{4.7}$$

where $\overline{\mathbf{n}} = \overline{\mathbf{S}}/S$.

5. Numerical solution

5.1. *Numerical integration of constitutive relations (Gauss point level)*

To approximate the value of any function y in the vicinity of certain point where it is equal to y_0, one can adopt the general form of the well-known trapezoidal operator such as the relation

$$y = y_0 + t[(1-\Theta)f(y_0,0) + \Theta f(y,t)], \tag{5.1}$$

for $0 \leq \Theta \leq 1$, where t represents the time interval and f – the time derivative of y. Using the limit values of Θ we arrive at the so-called fully implicit (for $\Theta = 1$) or fully explicit (for $\Theta = 0$) estimates, respectively. Particular application of this trapezoidal operator produces the following numerical approximation of Kirchhoff stresses

$$\overline{\mathbf{T}}_{n+1} = \overline{\mathbf{T}}_n + t\left[(1-\Theta)\dot{\overline{\mathbf{T}}}_n + \Theta\dot{\overline{\mathbf{T}}}_{n+1}\right], \tag{5.2}$$

where subscripts n and $n+1$ denote the two neighbouring states. Assuming the evolution of stresses as in (4.1) and viscoplastic rate of deformation as (4.2) in (5.2) for 3–D case, one can arrive at

$$\overline{\mathbf{T}}_{n+1} = \overbrace{\overline{\mathbf{T}}_n + 2G\Delta\overline{\boldsymbol{\epsilon}} + k\Delta e\cdot\mathbf{1}}^{\overline{\mathbf{T}}^{\mathrm{pre}}_{n+1}} - 2G\cdot t(1-\Theta)\dot{\gamma}^{vp}_n\overline{\mathbf{n}}_n - 2Gt\Theta\dot{\gamma}^{vp}_{n+1}\cdot\overline{\mathbf{n}}_{n+1}, \qquad 0\leq\Theta\leq 1, \tag{5.3}$$

where $\Delta\overline{\boldsymbol{\epsilon}} = \overline{\mathbf{D}}\cdot t$, $\mathrm{tr}(\overline{\mathbf{D}})\cdot t = \mathrm{tr}(\Delta\overline{\boldsymbol{\epsilon}}) = \Delta e$ and $\dot{\gamma}^{vp}_n = \varphi\langle\phi_n(\,\cdot\,)\rangle$. If we apply the full backward operator ($\Theta = 1$), and after the decomposition of Kirchhoff trial (elastic predictor) stresses into deviatoric and mean pressure components, we obtain

$$\begin{aligned}\overline{\mathbf{S}}_{n+1} &= \overline{\mathbf{S}}^{\mathrm{pre}}_{n+1} - 2Gt\dot{\gamma}^{vp}_{n+1}\cdot\overline{\mathbf{n}}_{n+1},\\ \overline{p}_{n+1} &= \overline{p}^{\mathrm{pre}}_{n+1} + k\Delta e^{vp}.\end{aligned} \tag{5.4}$$

The first trial (elastic predictor) step of numerical algorithm gives

$$\begin{aligned}\overline{\mathbf{T}}^{\mathrm{pre}}_{n+1} &= \overline{\mathbf{T}}_n + 2G\Delta\overline{\boldsymbol{\epsilon}} + k\Delta e\mathbf{1},\\ \overline{\mathbf{S}}^{\mathrm{pre}}_{n+1} &= \overline{\mathbf{S}}_n + 2G\Delta\overline{\boldsymbol{\epsilon}},\\ p^{\mathrm{pre}}_{n+1} &= p_n - k\Delta e.\end{aligned} \tag{5.5}$$

Evaluating the estimation of porosity and using the same way as before (backward operator), we arrive at

$$\eta^p_{n+1} = \eta^p_n - \eta\cdot t\cdot\mathrm{tr}\left(\overline{\mathbf{D}}\right) = \eta^p_n - \eta\Delta e, \tag{5.6}$$

where η could be obtained directly from the evolution law $\dot{\eta} = -\eta \operatorname{tr} \overline{\mathbf{D}}$ by exact integration. So we have

$$\eta = \eta_0 e^{-\Delta e}. \tag{5.7}$$

It is more convenient to present the last result in terms of p^{pre}_{n+1}, then in the short form Δe using the last equation of (5.6). Then the evolution of porosity η has the form as follows

$$\eta_{n+1} = \eta_n \cdot e^{(p^{\text{pre}}_{n+1} - p_n)/k}. \tag{5.8}$$

Instead of cumbersome integration, the problem reduces now to the solution of the following nonlinear system of equations

$$\begin{aligned} \overline{\mathbf{S}}_{n+1} &= \overline{\mathbf{S}}^{\text{pre}}_{n+1} - 2Gt\varphi\langle\phi_{n+1}(\,\cdot\,)\rangle\overline{\mathbf{n}}_{n+1}, \\ p_{n+1} &= p^{\text{pre}}_{n+1} + k\Delta e^{vp}, \\ \eta_{n+1} &= \eta_n e^{(p^{\text{pre}}_{n+1} - p_n)/k}. \end{aligned} \tag{5.9}$$

Let .us observe that after multiplication of the first equation of the above system by $\overline{\mathbf{n}}_{n+1}$, we arrive at the purely algebraic following system of equations

$$\begin{aligned} \overline{S}_{n+1} &= \overline{S}^{\text{pre}}_{n+1} - 2Gt\varphi\langle\phi_{n+1}(\,\cdot\,)\rangle, \\ \overline{p}_{n+1} &= \overline{p}^{\text{pre}}_{n+1} + k\Delta e^{vp}_{n+1}, \\ \eta_{n+1} &= \eta_n e^{(p^{\text{pre}}_{n+1} - p_n)/k}. \end{aligned} \tag{5.10}$$

The last equation of (5.10) can be directly used in Eqs. $(5.10)_1$ and $(5.10)_2$ because ϕ_{n+1} is the function of η_{n+1} and also $\Delta e^{vp}_{n+1} = \operatorname{tr}(\Delta\overline{\boldsymbol{\epsilon}}^{vp}) = t \cdot \operatorname{tr}(\overline{\mathbf{D}}^{vp}) = t \cdot \operatorname{tr}\left(\varphi\langle\phi(\,\cdot\,)\rangle \dfrac{\partial\phi}{\partial\mathbf{T}}\right)$, so finally we will use the system of only two algebraic equations.

The system of equations, which has to be solved at each integration point at all iterations, can be highly nonlinear, so we have to be sure that we are able to obtain a good convergence of results for a wide class of nonlinear expressions. For this purpose the BROWN solver [9] of nonlinear system of algebraic equations was tested for a lot of sophisticated functions, and finally applied to the general elastic predictor – plastic corrector algorithm. It was numerically proven that even for very difficult and almost singular nonlinear functions, starting from the arbitrary point the solver achieved the solution with good accuracy after only a few iterations. One can imagine, that the efficiency of this solver, which has to be used several times at each integration point and at each increment, is crucial for the finite element calculations. According to the numerical experience collected with this solver, we have never observed any difficulties with its convergence.

This integration procedure which is performed on the level of the Gauss point was included into the definition of the user subroutine UMAT that includes users own constitutive law in the commercial program ABAQUS [1]. In this case ABAQUS serves as the finite element framework to the solution of nonlinear mechanical problem. This attractive possibility which allows to include our own material law through subroutine UMAT requires the definition of the constitutive Jacobian matrix. It can influence the speed of convergence, for example the quadratic one, if a consistent linearization is used; (see Sec. 6). In the other formulations of constitutive Jacobian matrix one can expect a slower convergence, but it should not influence the lack of generally convergent properties of the algorithm. The summary of the main steps of constitutive algorithm is shown in Box 2.

Box 2

Summary of the constitutive algorithm

1. Calculate the trial stress and normal mean pressure

$$\overline{\mathbf{T}}_{n+1}^{\mathrm{pre}} = \mathbf{T}_n + \mathscr{C}[\Delta E_{n+1}], \qquad p_{n+1}^{\mathrm{pre}} = -\frac{1}{3}\mathrm{tr}(\overline{\mathbf{T}}_{n+1}^{\mathrm{pre}})$$

2. Deviatoric trial

$$\overline{\mathbf{S}}_{n+1}^{\mathrm{pre}} = \overline{\mathbf{T}}_{n+1}^{\mathrm{pre}} + p_{n+1}^{\mathrm{pre}}\mathbf{I}$$

3. If $\Phi(\cdot) \leq 0$ then the deformation is elastic
   the constitutive algorithm is complete
   else
   continue
4. Solve the system of algebraic equations (Eqs. (5.10))
5. Calculate the radial return factor λ_{n+1}
6. Update stresses

$$\overline{\mathbf{T}}_{n+1} = \lambda_{n+1}\overline{\mathbf{S}}_{n+1}^{\mathrm{pre}} + p_{n+1}^{\mathrm{pre}}\mathbf{I},$$
$$\mathbf{T}_{n+1} = \mathbf{Q}_{n+1}\overline{\mathbf{T}}_{n+1}\mathbf{Q}_{n+1}^{T}.$$

5.2. Numerical integration of the equations. Level of BVP

The method of regularization which is used in the paper, namely the viscoplastic one, requires fully dynamical formulation. ABAQUS offers the dynamic analyses both the explicit and implicit operators to solve the incremental problem. Explicit schemes determine the values of quantities at time t_{n+1} based on the available values at time t_n, but the procedure is

only conditionally stable and the length of time increment that defines the stability limit is approximately equal to the time for an elastic wave to cross the smallest element dimension in the model. Implicit schemes remove this bound on the time step size but nonlinear system of equations has to be solved. Usually in structural problems, implicit integration schemes give good solutions with the time steps by one or two orders of magnitude larger than the stability limits of the explicit version. In the finite element calculations of the dynamic boundary value problems we have used the wide spectrum of ABAQUS possibilities.

6. Consistent Jacobian matrix

In the finite element procedures which use the nonlinear constitutive model the weak form of the equilibrium equation is used to describe incremental motion which serves to calculate the values of stresses $\mathbf{T}$ and porosity η at the end of the increment. If these values do not satisfy the balance equations at the end of the increment, the iterative procedure starts and is continued until these requirements are fulfilled to within the assumed tolerances. As it was emphasized by Hughes [12], the *Consistent Jacobian Matrices* are used only in searching for the incremental motion, but have no effect on the final accuracy of the solution. However, in order to speed up the convergence (quadratic is characteristic for Newtonian methods), it is important to evaluate accurately this linearized form (see Nagtegaal and Veldpaus [23]).

For 2–D plane strain case the *Consistent Linearized Constitutive Operator* $\mathbf{J}$ of our visco-plastic, density-dependent soil-like model is

$$\mathbf{J} = \frac{d\Delta\overline{\mathbf{T}}}{d\Delta\mathbf{E}}, \tag{6.1}$$

where $\mathbf{C} = 2G\mathbf{I} + (k - G)\mathbf{1} \otimes \mathbf{1}$ is used. The following notation, where E is Young's modulus and ν is Poisson's ratio is adopted in the formulae

$$G = \frac{E}{2(1+\nu)}, \qquad K = \frac{E}{3(1-2\nu)},$$

$$k = K + \frac{1}{3}G = \frac{E}{2(1-2\nu)(1+\nu)}, \tag{6.2}$$

$$\Delta\gamma = \varphi\langle\phi\rangle t, \qquad \overline{\mathbf{n}} = \frac{\overline{\mathbf{S}}}{S}, \qquad a = \varphi\langle\phi\rangle,$$

where t denotes the increment of time.

Finally we obtain

$$\mathbf{J} = C_1^{vp}\mathbf{I} + C_2^{vp}\mathbf{1}\otimes\mathbf{1} + C_3^{vp}\overline{\mathbf{n}}\otimes\overline{\mathbf{n}} + C_4^{vp}\mathbf{1}\otimes\overline{\mathbf{n}} + C_5^{vp}\overline{\mathbf{n}}\otimes\mathbf{1}, \tag{6.3}$$

where the coefficients C_i^{vp} have the form

$$\begin{aligned}
C_1^{vp} &= 2G(1 - a\frac{2G}{S}\Delta\gamma),\\
C_2^{vp} &= k - G + \frac{a}{2S}(2G)^2\Delta\gamma + k^2 a\frac{\partial\Delta e^p}{\partial p} + \eta\frac{\partial\Phi}{\partial p}2kG\Delta e^p,\\
C_3^{vp} &= -(2G)^2 a\frac{\partial\Delta\gamma}{\partial S} + (2G)^2 a\frac{\Delta\gamma}{S} - \eta\frac{\partial\Phi}{\partial S}2G\Delta\gamma,\\
C_4^{vp} &= -2Gka\frac{\partial\Delta e^p}{\partial S} - \eta\frac{\partial\Phi}{\partial S}2Gk\Delta e^p,\\
C_5^{vp} &= 2Gka\frac{\partial\Delta\gamma}{\partial p} + \eta 2Gk\frac{\partial\Phi}{\partial p}\Delta\gamma.
\end{aligned} \tag{6.4}$$

7. Numerical examples

Let us examine a set of examples concerning a 10 m by 10 m pillar problem treated as a 2–D plane strain case under different mesh density. Basically we will use three meshes 10*10, 20*20 and 40*40 of rectangular elements of a linear shape functions. The results for both the rate-independent (without regularization) and rate-dependent models are presented and discussed. We will show the critical mesh dependence (sensitivity) of the first order for a rate-independent model in static or dynamic cases, and significant improvement of the results by using regularized viscoplastic dynamic formulation.

The interpretation of the mesh dependence is, according to Życzkowski's classification [40], presented on the level of structure (force-displacement space) and on the level of point (distribution of the equivalent plastic strains $\tilde{\varepsilon}^{pl} = \int\sqrt{\frac{2}{3}\mathbf{D}^p : \mathbf{D}^p}\,dt$).

The data accepted according to Drescher [6] in the finite element calculations reflect the parameters for medium granular sand: $E = 29.4$ MPa, $\nu = 0.3$, $\alpha = 4.905$, $n = 0.58$, $c_0 = 7.8$, $\eta_0 = 1.64\,\mathrm{g/m^3}$.

The results presented here concern mainly the 4 node bi-linear reduced-integration elements with hourglass control.

7.1. Rate-independent model

The purpose of presenting the results for non-regularized (rate-independent) model is to gain the numerical evidence of the significant sensitivity of the final results to the mesh used in computations.

7.1.1. Statics. Let us consider the boundary value problem of a pillar presented in Fig. 1, and assume the perfect interaction of the specimen with the rigid plates on its top and bottom sides. Let us assume also the displacement-controlled process in such a way that the top side moves down preserving the same displacements of all its nodes. Arc-length method was used to control the incremental process.

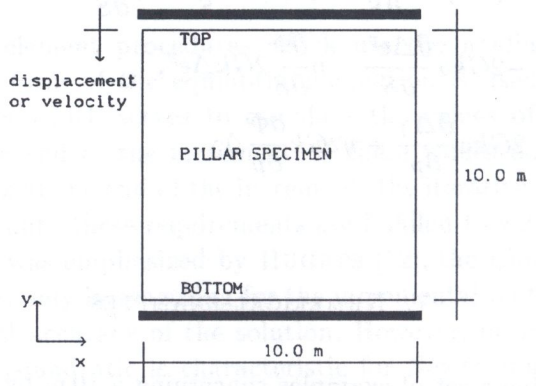

FIG. 1. Two-dimensional plane strain pillar problem.

Concentration of the plastic deformation is clearly visible along the diagonals of the pillar. The results of plastic shear strains for different types of elements CPE4 (linear 4-node quadrilateral element) and CPE4R (bi-linear 4-node with reduced integration quadrilateral) obtained under 10*10 elements discretization are presented in Fig. 2a. We can compare the concentration of plastic strains with the results obtained for 20*20 mesh (Fig. 2b).

It is natural that for this rate-independent formulation, the width of localization should tend to zero. The tendency observed in numerical experiments confirms this expectation and shows more concentrated strains around the diagonals for finer meshes. The confirmation of a strong mesh sensitivity on the global level is shown in Fig. 3, where the diagram of the total forces versus the displacement of the top side of the pillar is plotted. For the static case, the different meshes used in the calculations lead to different behaviour in the post-critical states (after the peak load has been reached), and also predict different maximal values of forces that the structure can carry.

a) Plastic Shear Strain, t=0.432, CPE4

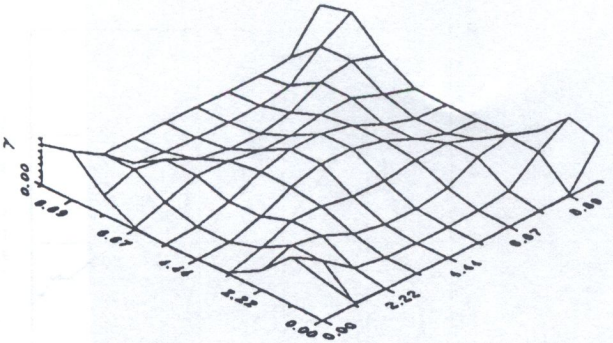

Plastic Shear Strain, t=0.430, CPE4R

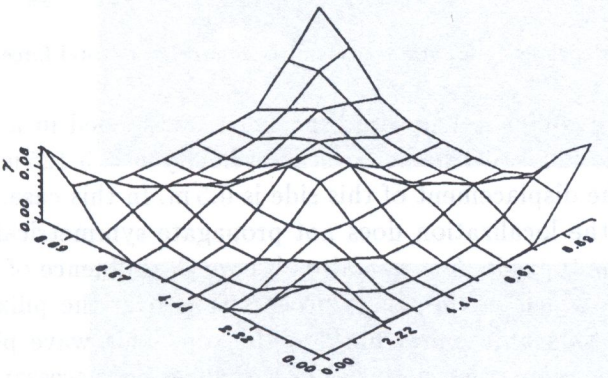

b) Plastic Shear Strain, t=0.430, CPE4

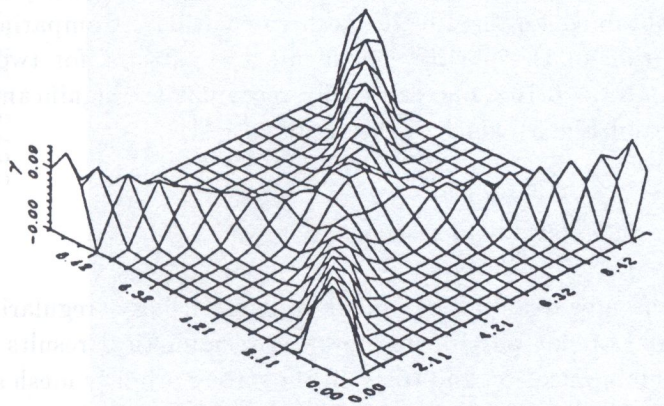

FIG. 2. Distribution of plastic shear strain under static loading for 10*10 meshes and 20*20 mesh; a) CPE4 (bi-linear elements) and CPE4R (bi-linear elements with reduced integration) 10*10 meshes, b) CPE4 (bi-linear elements) 20*20 mesh.

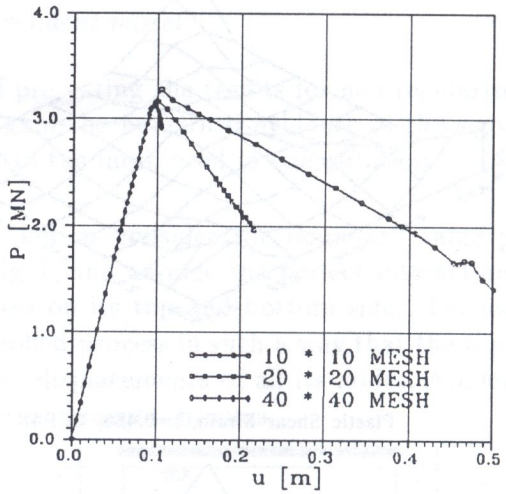

FIG. 3. Mesh dependence for static case on the global level. Total force vs. displacements.

7.1.2. Dynamics. The same specimen was loaded in a dynamical way. The top side moves with the constant velocity $v = 3.125\,\mathrm{m/s}$ so that after $t = 0.16\,\mathrm{s}$ the displacement of this side is 0.5 m. In this case, contrary to the static one, the localization does not propagate symmetrically but it starts first from the top side. One can also observe the influence of the elastic wave propagation which in the whole process runs over the pillar, reflects from the bottom side and comes back to the top. This wave plays the role of imperfection, so no other artificial disturbances are necessary to enforce the place of localization.

In Fig. 4 we can observe the development of equivalent plastic shear strain zones obtained for the 40*40 mesh calculations. Comparing the results of distribution of the plastic equivalent shear strains for two meshes at the same time $t = 0.16\,\mathrm{s}$, one can easily recognize the significant difference (see Fig. 4d and Fig. 5) which is the result of PMD.

7.2. Rate-dependent viscoplastic model

Let us now examine our pillar problem using a regularized model. The main goal of this part of presentation of numerical results is to show the effect of minimization and to avoid the strong primary mesh sensitivity. Only the dynamical calculations are taken into consideration and the conditions are such as those defined in Sec. 7.1.1. The relaxation time which was used in calculations was of the order of $T_m = 10^{-3}\,\mathrm{s}$. In Fig. 6 we present the distribution of the plastic equivalent strains for two meshes of 10*10 and

a)

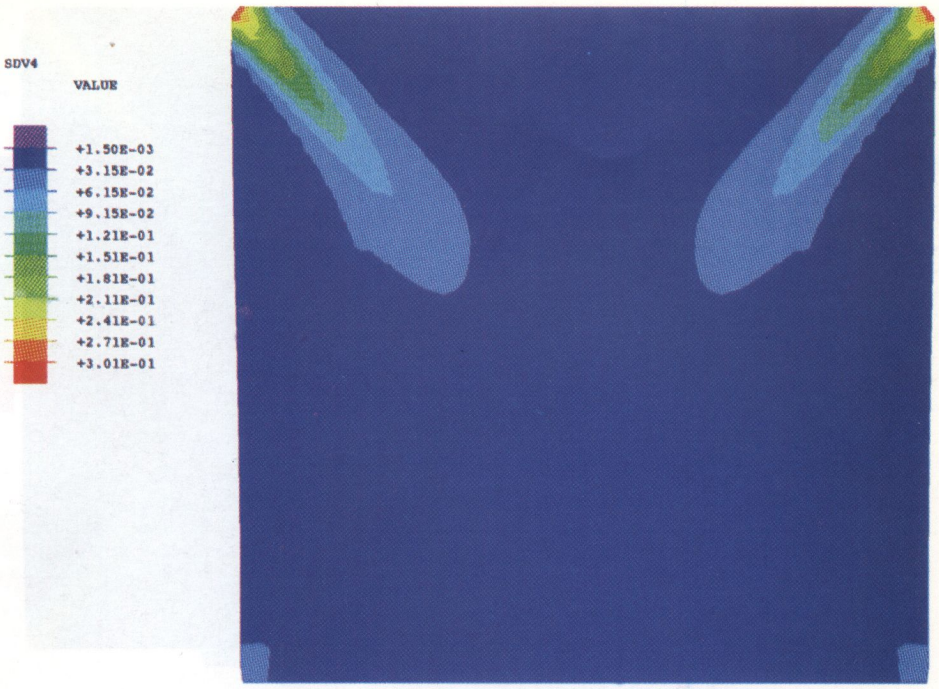
SDV4
VALUE
+1.50E-03
+3.15E-02
+6.15E-02
+9.15E-02
+1.21E-01
+1.51E-01
+1.81E-01
+2.11E-01
+2.41E-01
+2.71E-01
+3.01E-01

b)

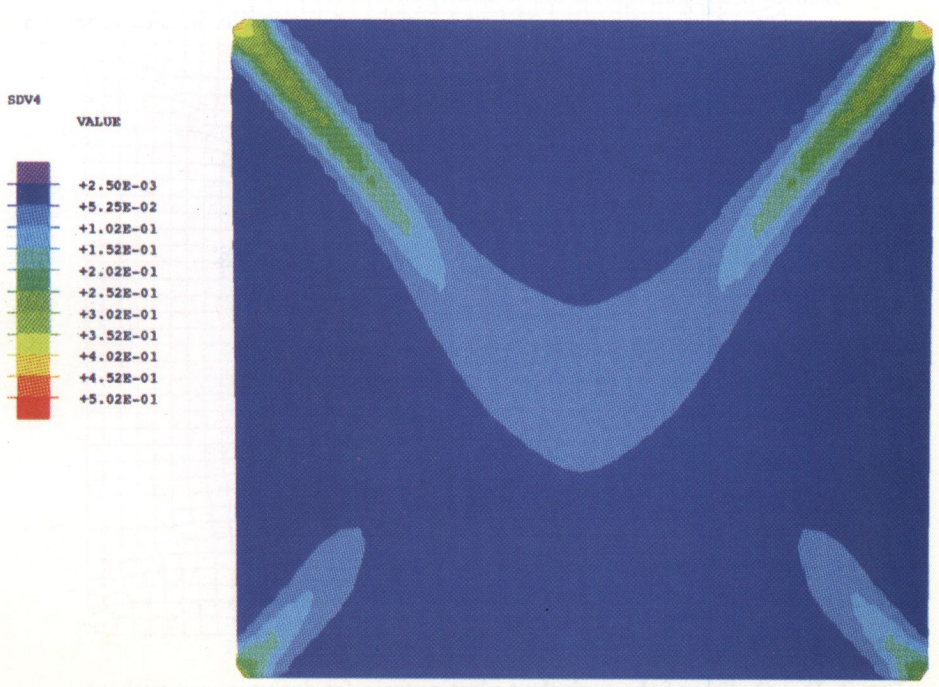
SDV4
VALUE
+2.50E-03
+5.25E-02
+1.02E-01
+1.52E-01
+2.02E-01
+2.52E-01
+3.02E-01
+3.52E-01
+4.02E-01
+4.52E-01
+5.02E-01

[FIG. 4 a, b]

c)

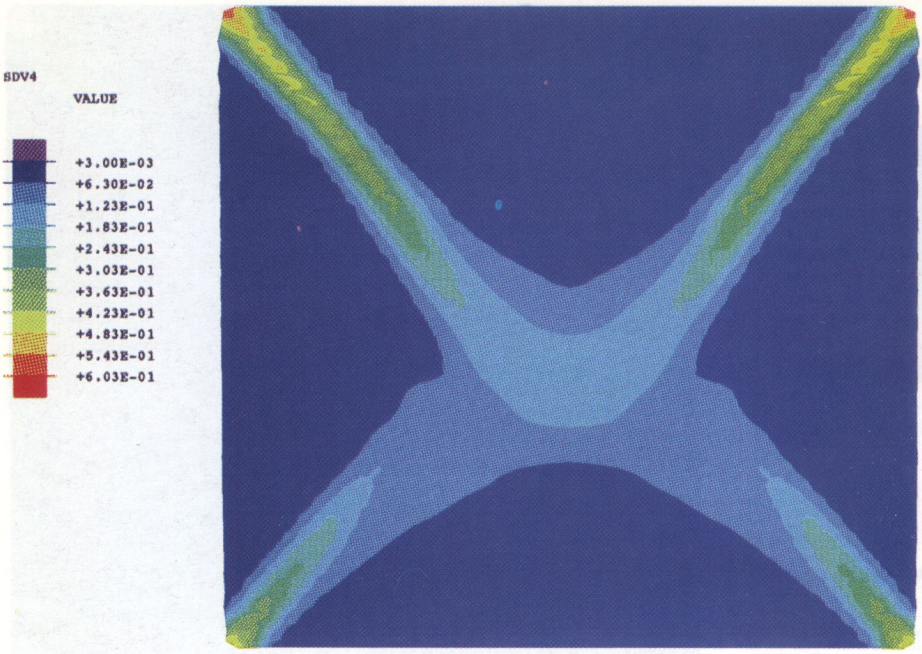

d)

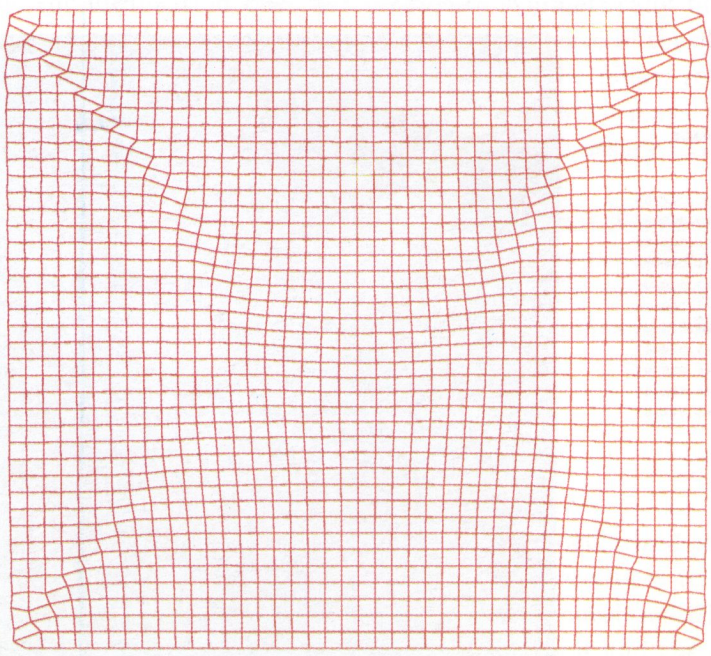

FIG. 4. Distribution of the equivalent plastic strain for dynamic case without regularization for $40 * 40$ mesh. Development of localized strains zones in time: a) $t = 0.08\,\mathrm{s}$, b) $t = 0.12\,\mathrm{s}$, c) $t = 0.16\,\mathrm{s}$; d) deformed mesh. The assumed velocity of movement of the top side $v = 3.125\,\mathrm{m/s}$.

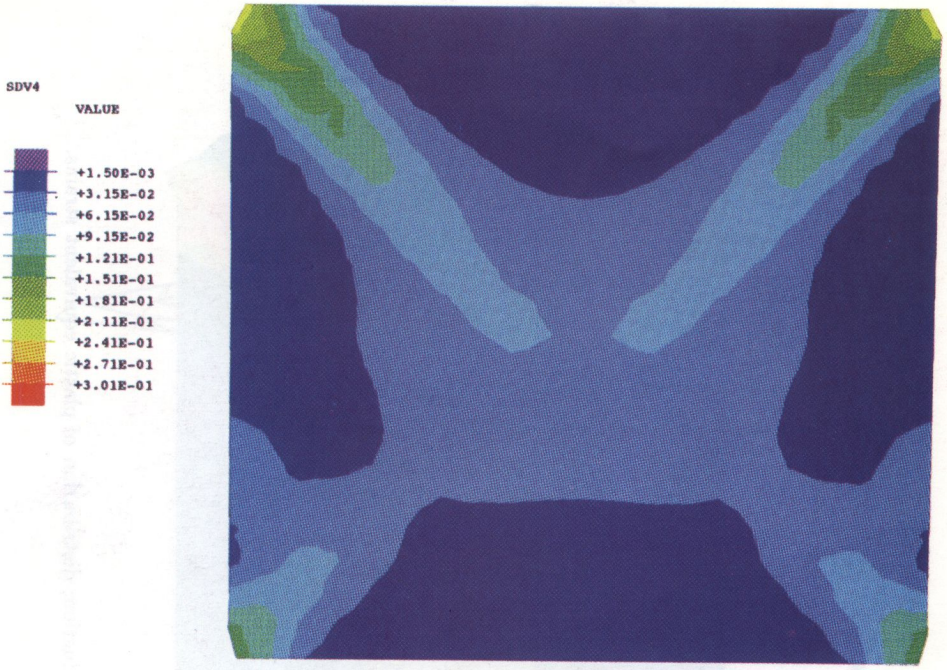

FIG. 5. Distribution of the equivalent plastic strain for dynamic case without regularization for $20 * 20$ mesh and $t = 0.16\,\mathrm{s}$. (For comparison with Fig. 4 c).

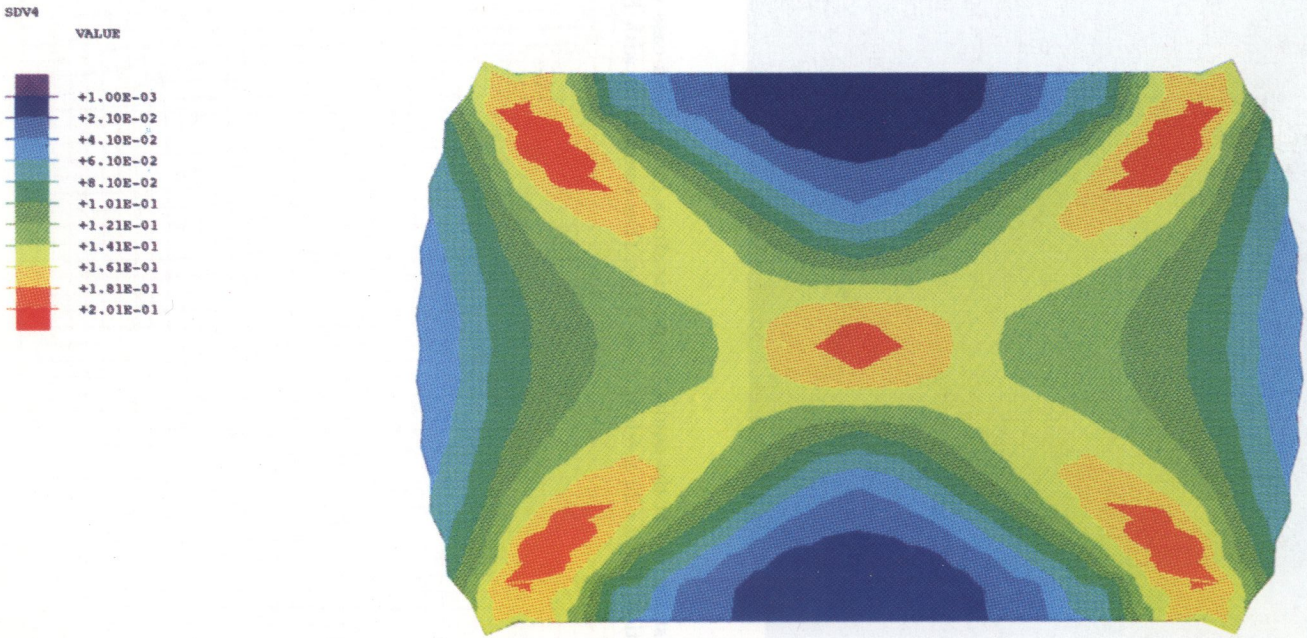

FIG. 9. Large displacement analysis. Final state 40% of depth reduction; distribution of plastic equivalent strains.

a)

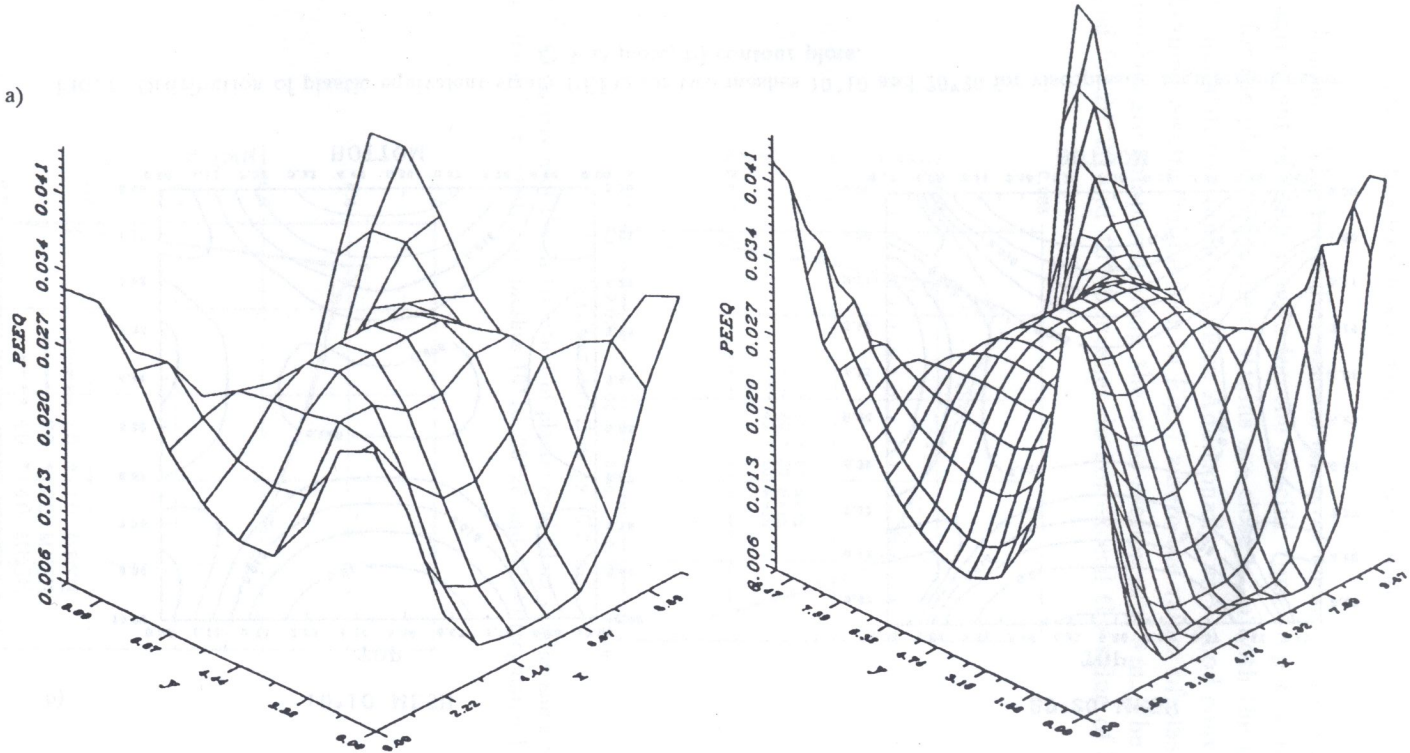
PEEQ
0.006
0.013
0.020
0.027
0.034
0.041
Y
X
PEEQ
0.006
0.013
0.020
0.027
0.034
0.041
Y
X

[FIG. 6a]

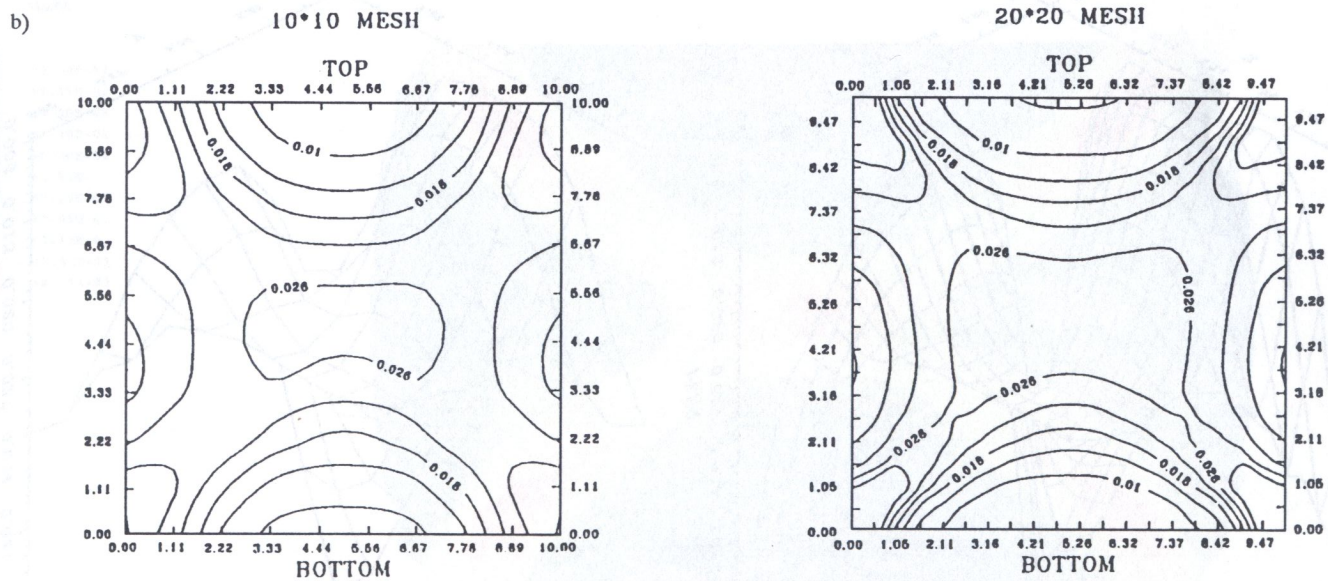

FIG. 6. Distribution of plastic equivalent strain PEEQ for two meshes 10*10 and 20*20 for viscoplastic regularized cases; a) 3–D plots, b) contour plots.

20*20 elements. The three-dimensional plots of these strains confirm the good agreement of both results for the specific time step $t = 0.16\,\mathrm{s}$. The results for the plastic equivalent strains are close from both the qualitative and the quantitative points of view. Additionally, very good convergence of the obtained results can be seen in Fig. 7 where the values of plastic strains for 3 meshes are compared along the cross-section $x = 8\,\mathrm{m}$. The difference obtained for 20*20 and 40*40 meshes do not exceed the value of 5%.

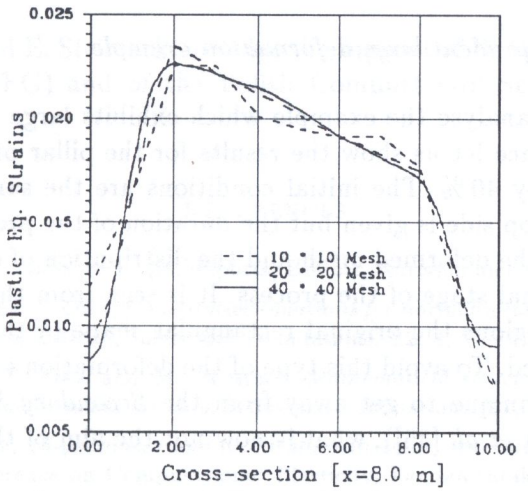

FIG. 7. Comparison of the distribution of plastic equivalent strains along the pillar specimen for $x = 8.0\,\mathrm{m}$ for meshes 10*10, 20*20 and 40*40 (regularized case).

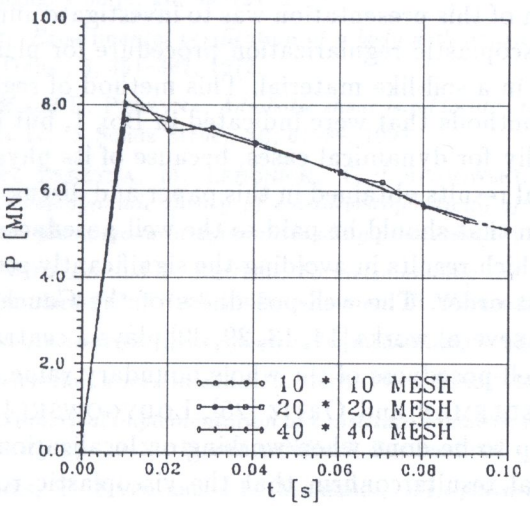

FIG. 8. The effect of viscoplastic regularization for dynamic case total force vs. time (velocity driven problem).

One can observe that for a viscoplastic model the localization zones are diffused. Their widths do not tend to singular lines like those for rate-independent models. The degree of diffusion of those zones depends significantly on the viscosity (relaxation time) used in calculations.

In Fig. 8 we present the result of the viscoplastic regularization in the space of forces and displacements for which the effect of reduction of the *Primary Mesh Dependence* PMD is evident.

7.3. Rate-dependent large deformation example

Now we can analyse the example which exhibits large deformations. As numerical evidence let us show the results for the pillar problem, its depth being reduced by 40%. The initial conditions are the same as before, i.e. velocity of the top side is given but the duration of the process is extended. Figure 9 shows the deformed mesh and the distribution of equivalent plastic strains at the final stage of the process. It is seen from the deformed mesh that for some regions the original rectangular shape of the elements is significantly changed. To avoid this type of the deformation one should include an adaptive technique to get away from the *Secondary Mesh Dependence* SMD (see STEIN *et al.* [35]), what is now not the aim of this presentation.

8. CONCLUSIONS AND FINAL REMARKS

The main aim of this presentation was to investigate numerically the possibility of the viscoplastic regularization procedure for plastic flow localization phenomena in a soil-like material. This method of regularization is one of the possible methods that were indicated in Box 1, but it seems to be attractive, especially for dynamical cases, because of its physical justification.

The numerical results obtained in this paper and discussed herein emphasize the attention that should be paid to the well-posedness of the boundary value problem which results in avoiding the significantly strong mesh dependence of the first order. The well-posedness of the Cauchy problem which was discussed in several works [14, 13, 29, 30] plays a central role but it does not assure the well-posedness of the whole boundary value problem (see BENALLAL [4], NEEDLEMAN and ORTIZ [25], ŁODYGOWSKI [19]), nevertheless it is the first step to be done when working on localization problems.

The numerical results confirm that the viscoplastic regularization procedure of plastic flow used here is an efficient computational tool for the description and numerical calculation of localization of plastic strains.

Particularly, in the examples presented in this paper, a significant reduction of the so-called *Primary Mesh Dependence* PMD, as the result of mathematical well-posedness via viscoplasticity, is clearly demonstrated.

Acknowledgment

The support of KBN grant 7-TO7-A013-10 is gratefully acknowledged (T.Ł.).

P. Perzyna and E. Stein acknowledge the support of Deutsche Forschungsgemeinschaft (DFG) and of the Polish Committee of Scientific Research (KBN).

References

1. *ABAQUS. Manuals for v. 4.9*, Reports, Hibbitt, Karlsson and Sorensen, Inc., 1990.
2. T. Adachi and F. Oka, *Constitutive equations for normally consolidated clay based on elasto-viscoplasticity*, Solids and Foundations, **22**, 4, 57–70, 1982.
3. T. Adachi, F. Oka and M. Mimura, *Mathematical structure of an overstress elasto-viscoplastic model for clay*, Solids and Foundations, **27**, 4, 31–42, 1987.
4. A. Benallal, *Ill-posedness and localisation in solid structures*, [in:] Proc. Third Intern. Conference on Computational Plasticity, Fundamentals and Applications, D.R.J. Owen, E. Onate and E. Hinton [Eds.], Barcelona, April 6–10, 1992, pp. 483–508, 1992.
5. R. de Borst, *Fundamental issues in finite element analyses of localization of deformation*, Engng. Comp., **10**, 99–121, 1993.
6. A. Drescher, *Experimental verification of a body with density hardening* [in Polish], Engng. Trans., **3**, 351–387, 1972.
7. M.K. Duszek and P. Perzyna, *Adiabatic shear band localization in elastic-plastic single crystals*, Int. J. Solids Struc., **30**, 61–89, 1993.
8. M.K. Duszek–Perzyna, M. Lengnick, T. Łodygowski, P. Perzyna and E. Stein, *Thermodynamic theory of elasto-viscoplasticity of geological materials and localization phenomena in dynamic loading processes* [in preparation].
9. G. Engeln–Müllges and F. Reuter, *Formelsammlung zur Numerischen Mathematik mit Standard-FORTRAN 77-Programmen*, BI Wissenschaftsverlag, 1988.
10. M.E. Gurtin, *An introduction to continuum mechanics*, Academic Press, 1981.
11. R. Hill, *Acceleration waves in solids*, J. Mech. Phys. Solids, **10**, 1–16, 1962.
12. T. Hughes, *Numerical implementation of constitutive models: rate-independent deviatoric plasticity*, pp. 29–57, Martinus Nijhoff, Boston 1984.
13. T.J.R. Hughes, T. Kato and J.E. Marsden, *Well-posed quasi-linear second-order hyperbolic systems with applications to nonlinear elastodynamics and general relativity*, Arch. Rat. Mech. Anal., **63**, 273–294, 1977.

14. T. KATO, *The Cauchy problem for quasi-linear symmetric hyperbolic systems*, Arch. Rational Mech. Anal., **58**, 181–205, 1975.

15. K. KIBLER, M. LENGNICK and T. ŁODYGOWSKI, *Selected aspects of the well-posedness of the localized plastic flow processes*, CAMES [submitted for publication].

16. E.H. LEE, *Elastic-plastic deformations at finite strains*, J. Appl. Mech., **36**, 1969.

17. S. LEROUEIL, M. KOBBAJ, F. TAVENAS and R. BOUCHARD, *Stress-strain-strain rate relation for the compressibility of sensitive natural clays*, Geotechnique, **35**, 159–180, 1985.

18. T. ŁODYGOWSKI, *Mesh-independent beam elements for strain localization*, Meth. in Civil Engng., **3**, 3, 9–24, 1993.

19. T. ŁODYGOWSKI, *Theoretical and numerical aspects of plastic strain localization*, Wyd. Rozprawy Politechniki Poznańskiej, Nr 312, 1996.

20. T. ŁODYGOWSKI, *On avoiding of spurious mesh sensitivity in numerical analysis of plastic strain localization*, CAMES, **2**, 3, 231–248, 1995.

21. B. LORET, *An introduction to classical theory of elastoplasticity*, [in:] Geomaterials: constitutive equations and modelling, F. DARVE [Ed.], pp. 149–186, Elsevier Applied Science, London and New York 1990.

22. J. MANDEL, *Conditions de stabilité et postulat de Drucker*, [in:] Rheology and Soil Mechanics, J. KRAVTCHENKO and P.M. SIRIEYS [Eds.], pp. 58–68, Springer, Berlin 1966.

23. J.C. NAGTEGAAL and F.E. VELDPAUS, *On the implementation of finite strain plasticity equations in a numerical model*, [in:] Numerical analysis of forming processes, J.F.T. PITMAN, O.C. ZIENKIEWICZ, R.D. WOOD and J.M. ALEXANDER [Eds.], John Wiley and Sons Ltd., 1984.

24. A, NEEDLEMAN, *Material rate dependence and mesh sensitivity in localization problems*, Comp. Meth. in Appl. Mech. Engng., **67**, 69–85, 1988.

25. A, NEEDLEMAN and M. ORTIZ, *Effect of boundaries and interfaces on shear–band localization*, Int. J. Solids Struc., **28**, 7, 859–877, 1991.

26. P. PERZYNA, *The constitutive equations for rate sensitive plastic materials*, Quart. Appl. Math., **20**, 321–332, 1963.

27. P. PERZYNA, *Fundamental problems in viscoplasticity*, [in:] Advances in Applied Mechanics, C.-S. YIH [Ed.], **9**, pp. 243–377, Academic Press, 1966.

28. P. PERZYNA, *Thermodynamic theory of viscoplasticity*, [in:] Advances in Applied Mechanics, **11**, pp. 313–354, Academic Press, 1971.

29. P. PERZYNA, *Constitutive equations of dynamic plasticity*, [in:] Computational Plasticity, Fundamentals and Applications, D.R.J. OWEN, E. OÑATE and E. HINTON [Eds.], Swansea, Barcelona, April 6-10, 1992, Pineridge Press, pp. 483–508, 1992.

30. P. PERZYNA, *Analysis of the fundamental equations describing thermoplastic flow process in solid body*, Arch. Mech., **43**, 287–296, 1993.

31. S. PIETRUSZCZAK and Z. MRÓZ, *Numerical analysis of elastic–plastic compression of pillars accounting for material hardening and softening*, Int. J. Rock Mech. Min. Sci. Geomech., **17**, 199–207, 1980.

32. J.R. RICE, *The localization of plastic deformation*, [in:] Theoretical and Applied Mechanics, W.T. KOITER [Ed.], pp. 207–220, North-Holland Publishing Company, 1976.

33. J.W. RUDNICKI and J.R. RICE, *Conditions for the localization of deformations in pressure-sensitive dilatant meterials*, J. Mech. Phys. of Solids, **23**, 371–394, 1975.

34. L.J. SLUYS, J. BLOCK and R. DE BORST, *Wave propagation and localization in viscoplastic media*, [in:] Int. Conf. on Comp. Plasticity, Fundamentals and Applications, COMPLAS III, Barcelona, Spain, April 4-9, 1992, E. HINTON D. OWEN, E. OÑATE [Eds.], pp. 539–550, 1992.

35. E. STEIN, S. OHNIMUS, B. SEIFERT and R. MAHNKEN, *Adaptive Finite-Element Diskretisirungen von Flächentragwerken*, Bauingenieur [in press], 1993.

36. F. TAVENAS and S. LEROUEIL, *The behaviour of embankments on clay foundations*, Canadian Geotech. J., **17**, 236–260, 1980.

37. F. TAVENAS, S. LEROUEIL, P. LA ROCHELLE and M. ROY, *Creep behaviour of an undisturbed lightly overconsolidated clay*, Canadian Geotech. J., **15**, 402–423, 1978.

38. C. TRUESDELL and W. NOLL, *The nonlinear field theories*, [in:] Handbuch der Physik, Band III/3, Springer, Berlin, Heidelberg, New York 1965.

39. D.M. WOOD, *Soil behaviour and critical state soil mechanics*, Technical Report, Cambridge University Press, 1990.

40. M. ŻYCZKOWSKI, *Combined loadings in the theory of plasticity*, PWN, 1981.

INSTITUT FÜR BAUMECHANIK UND NUMERISCHE MECHANIK
UNIVERSITÄT HANNOVER, HANNOVER, GERMANY;
POZNAŃ UNIVERSITY OF TECHNOLOGY, POZNAŃ
and
POLISH ACADEMY OF SCIENCES
INSTITUTE OF FUNDAMENTAL TECHNOLOGICAL RESEARCH.

Received May 17, 1996.